Electrogenerated Chemiluminescence

XXXIII. The Production of Excited States by Direct Heterogeneous Electron Transfer from Semiconductor Electrodes

J. D. Luttmer* and Allen J. Bard**

Department of Chemistry, The University of Texas at Austin, Austin, Texas 78712

ABSTRACT

Electrogenerated chemiluminescence (ECL) arising from direct electron transfer from semiconductor electrodes to solution species was examined. The reduction of the oxidized forms of several luminescent species [$Ru(bipy)_3^{2+}$, thianthrene, 9,10-diphenylanthracene, and rubrene] on several n-type semiconductor electrodes (CdS, ZnO, TiO_2, SiC, GaP) was investigated. Only for reduction of rubrene radical cation on n-ZnO and n-CdS was unequivocal evidence found for production of an excited state (triplet) by direct heterogeneous electron transfer at potentials where homogeneous redox processes producing excited states were not possible. Current interruption techniques were employed to study the emission decay and an unusual emission at open circuit following a cathodic potential step was found. A model for direct triplet generation based on reduction via surface states within the bandgap region and quenching of excited states by the electrode is proposed and constraints on the experimental observation of direct excited state formation are suggested.

Many examples of the electrogenerated chemiluminescence (ECL) of aromatic molecules and rare earth chelates have been reported over the last decade and several reviews have been published (1-8). Usually these studies involve generating excited states (triplets and singlets) via homogeneous electron transfer between electrogenerated oxidized and reduced forms, frequently radical anions and cations ("radical ion annihilation"), *e.g.*, for rubrene (R)

$$R^{+\cdot} + R^{-\cdot} \rightarrow {}^3R^* + R \quad [1]$$

$${}^3R^* + {}^3R^* \rightarrow {}^1R^* + R \quad [2]$$

$${}^1R^* \rightarrow R + h\nu \quad [3]$$

or for $Ru(bipy)_3^{2+}$

$$Ru(bipy)_3^{3+} + Ru(bipy)_3^{+} \rightarrow {}^3Ru(bipy)_3^{2+*} + Ru(bipy)_3^{2+} \quad [4]$$

$${}^3Ru(bipy)_3^{2+*} \rightarrow Ru(bipy)_3^{2+} + h\nu' \quad [5]$$

Recent papers however have reported that excited states may also be formed by direct heterogeneous electron transfer at a semiconductor electrode surface (9, 10). Gleria and Memming (9) observed emission upon reduction of $Ru(bipy)_3^{3+}$ (bipy = 2,2'-bipyridine) at n-SiC and n-GaP semiconductor electrodes in H_2O or acetonitrile (ACN) solutions and proposed the reaction sequence

$$Ru(bipy)_3^{3+} + e^-(CB) \rightarrow {}^3Ru(bipy)_3^{2+*} \quad [6]$$

followed by [5], where $e^-(CB)$ represents an electron in the conductor band of the semiconductor. Yeh and Bard (10) reported singlet emission from rubrene produced by direct heterogeneous generation of the triplet state by reduction of $R^{+\cdot}$ at an n-ZnO electrode followed by triplet-triplet annihilation in benzene-benzonitrile mixed solvent. *i.e.*

$$R^{+\cdot} + e^-(CB) \rightarrow {}^3R^* \quad [7]$$

followed by [2] and [3]. In both studies it was proposed that the electron transferred from the conduction band to the oxidized solution species to form the excited triplet species. This is shown schematically in Fig. 1. Direct electron transfer to produce the ground state molecule should be less probable when the redox potential of the ground state molecule corresponds to an energy level within the bandgap of the semiconductor.

On a metal electrode an electron can be transferred from an isoenergetic state in the electrode to a lower orbital to produce the ground state of the molecule and no emission is expected. Moreover, excited state species are both more easily oxidized and more easily reduced at metal electrodes compared to the ground state species and metals are consequently good quenchers of excited states via electron transfer (11, 12). Quenching of excited state species by energy transfer to a metal is also well known (13). Although the direct heterogeneous production of triplet states at metal electrodes has been claimed (14), the emission observed in such cases has been attributed to a "preannihilation" type of ECL which involves reactions of impurities or electrogenerated products in the ECL solution (15, 16). Several other authors have been unable to observe evidence for the direct heterogeneous production of excited states on semiconductor

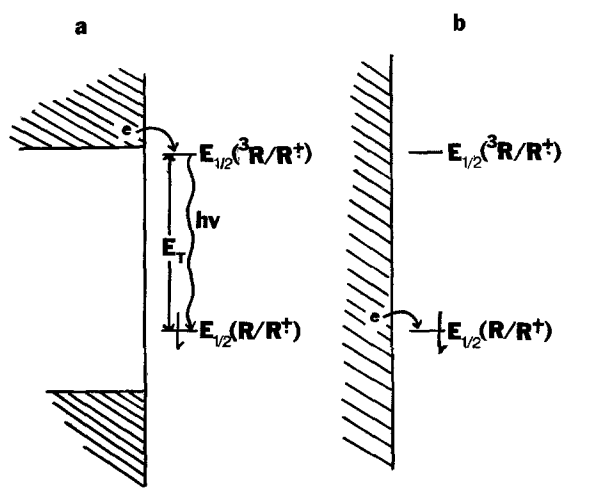

Fig. 1. Electron transfer from electrodes to oxidized solution species: (a) on a semiconductor, (b) on a metal electrode.

* Electrochemical Society Student Member.
** Electrochemical Society Active Member.
Key words: luminescence, energy transfer, organic, voltammetry.

electrodes (17, 18). Moreover, in the studies reporting the direct heterogeneous production of excited states at semiconductors a rigorous examination of the possibility of preannihilation ECL contributing to the observed emission and of the extent of ECL arising from a homogeneous electron transfer involving inadvertently generated reduced forms of the emitting species was not undertaken. We report here a more detailed study of the ECL emission mechanism in these systems and examine other possible systems for excited state production by direct heterogeneous electron transfer from semiconductor electrodes.

Experimental

Acetronitrile (ACN) (Spectro Grade, Matheson, Coleman, and Bell; MCB) was purified by repeated vacuum distillation from P_2O_5 and freeze-pump-thaw cycles to remove O_2 as described by Park and Bard (19). Benzonitrile (BZN; MCB) was fractionally distilled under partial vacuum from $CaSO_4$ and again from P_2O_5. It was then refluxed over, and fractionally distilled from, CaH_2 under high vacuum. Oxygen was removed by three freeze-pump-thaw cycles and the solution was stored over activated neutral alumina. Benzene (Spectro Grade MCB) was stored over a sodium mirror for more than one week, then was vacuum distilled, and underwent four freeze-pump-thaw cycles to remove O_2.

Tris (2,2′ bipyridyl) ruthenium (II) perchlorate, $[Ru(bipy)_3(ClO_4)_2]$ was prepared by metathesis of $Ru(bipy)_3Cl_2 \cdot 6H_2O$ (G. F. Smith) with excess $NaClO_4$ in H_2O. The crystals were washed with H_2O, recrystallized once from ethanol and twice from ACN, and dried under vacuum at 90°C for 24 hr. Thianthrene (TH) (Aldrich) was recrystallized twice from benzene and sublimed. Rubrene (R) (Aldrich) was recrystallized three times from xylene-methanol under nitrogen in subdued light and dried under vacuum at 80°C. 9,10-Diphenylanthracene (DPA) (Gold Label, Aldrich) was recrystallized from xylene-methanol, sublimed, and zone refined.

Tetra-n-butylammonium perchlorate (TBAP) (Polarographic Grade, Southwestern Analytical Chemicals) was purified by filtering a warm ethanolic solution of the electrolyte containing activated carbon and repeated recrystallization from an ethanol-water mixture. A final recrystallization was done from benzene and the crystals were dried under vacuum at 50°C for 36 hr. All samples, solvents, and electrolytes were transferred to a Vacuum Atmospheres dry box in which the solutions were prepared and the electrochemical/ECL cells were filled.

The n-type single crystal semiconductor electrodes were prepared and mounted as previously described (20, 21). Ohmic contacts were made to them by electrodepositing indium on one side and attaching a lead with silver-epoxy cement. Silicone adhesive (Dow Corning) was used to insulate the electrical contact from the electrochemical solution. A platinum foil working electrode of similar area and geometry was fabricated in a similar manner. The electrodes were polished with 0.5 μm alumina and had geometric areas of 0.3-0.5 cm^2. N-CdS (National Lead) and n-GaP (Atomergic) were etched in 11M HCl for 30 sec. N-TiO_2 (National Lead) and n-SiC[1] were etched in an HF/HNO_3 mixture for 30 sec. N-ZnO (Atomergic) was first etched in H_3PO_4 and then in concentrated HCl, each for 15 sec. The flatband potentials of these semiconductor electrodes have previously been determined from the onset of the anodic photocurrent in ACN (9, 20, 21) and are given in Table I.

The electrochemical/ECL cell was of conventional design with the reference compartment separated by a porous Vycor (Corning Glass) glass plug and the auxiliary electrode separated by dual frits of medium porosity. The auxiliary electrode consisted of a very large piece of platinum foil or wire mesh. Controlled potential waveforms for ECL and cyclic voltammetry were obtained with a PAR Model 175 programmer and Model 173/176 potentiostat. Current-time and ECL intensity-time curves were obtained with a Nicolet 1090A digital oscilloscope and recorded on a Houston 2000 X-Y recorder. An Aminco-Bowman spectrophotofluorometer was used to obtain ECL and fluorescence spectra. The ECL and fluorescence detectors used were RCA 1P28 and RCA 4832 photomultiplier tubes incorporating an RCA 3140 operational amplifier as a current follower. The intensity response of the emission detectors was adjusted, as necessary, by the selected input sensitivity of the Nicolet oscilloscope or by expansion of the digitized data in the oscilloscope. The current interrupter, fabricated with a silicon p-channel field effect transistor (Archer, No. 276-2037) driven by a Wavetek Model 114 signal generator, had a switching time of less than 3 μsec. The oxidized form of the electroactive species studied was produced by partial (25-75%) *in situ* controlled potential bulk electrolysis of the solution (about 20 min) on a large platinum foil electrode prior to the ECL studies.

[1] Courtesy of Prof. R. Memming, Phillips Research Laboratories, Hamburg, Germany.

Table I. Semiconductor electrode properties

Electrode	E_g (eV)[a]	V_{fb}[b]
n-CdS	2.45	−0.85[c]
n-ZnO	3.1	−0.76[c]
n-TiO_2	3.2	−0.8[d]
n-GaP	2.25	−1.5[e]
nSiC	3.0	−1.5[e,f]

[a] Bandgap energy.
[b] Flatband potential, *V vs.* SCE in ACN.
[c] Ref. (21).
[d] Ref. (20).
[e] Ref. (22).
[f] P. Kohl, private communication.

Results

Experimental approach.—In demonstrating direct excited state production via heterogeneous electron transfer at the electrode care must be taken to assure that the emission does not arise from the homogeneous radical ion annihilation path (Eq. [1]-[5]) or from a "preannihilation" or impurity pathway. In this latter case emission arises from the electrogeneration of a reactant from a small amount of impurity (X). For example, if X is reducible the following sequence is possible

$$X + e \longrightarrow X^- \qquad [8]$$

$$X^- + R^+ \longrightarrow {}^3R + X \qquad [9]$$

followed by reactions [2] and [3]. Because light levels 10^{-3}-10^{-4} times below the annihilation level are detected readily, impurity concentrations at the 10^{-6}-$10^{-7}M$ level can contribute appreciable preannihilation emission. X can represent either an impurity initially present or one generated from a small amount of decomposition of R^+ (or other electrogenerated reactant in the ECL annihilation reaction). The possibility of these paths was not studied in depth in the previous investigation of ECL at semiconductor electrodes (9, 10).

The approach employed to distinguish the direct route from the annihilation and preannihilation paths involved examining the electrochemical behavior and emission observed with a platinum electrode (which we assume will not show direct excited state formation), under careful potential control, with that of the semiconductor electrode. A solution containing the oxidized precursor [*e.g.*, R^+ or $Ru(bipy)_3^{3+}$] was prepared and the potential of the working electrode was scanned linearly in a negative direction at 2

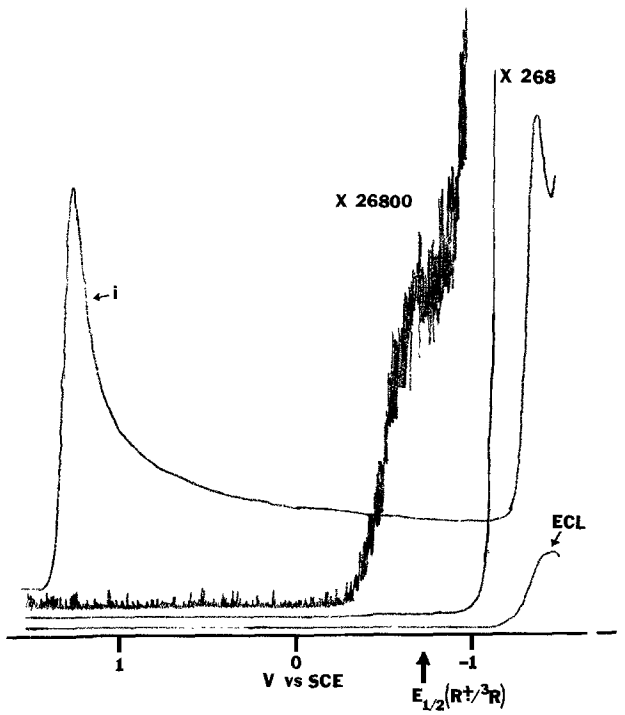

Fig. 2. ECL-potential and current-potential profiles obtained by cathodic potential scans at 2 V/sec 1.5 mmoles $Ru(bipy)_3^{3+}$ in 0.1M TBAP/ACN on platinum.

V/sec from potentials where the oxidized percursor was stable. Plots of the cathodic current (i) and the ECL intensity (I) as a function of potential (E) were thus obtained with different photomultiplier sensitivities. Typical results for a platinum electrode and $Ru(bipy)_3^{3+}$ in ACN/TBAP solution are shown in Fig. 2. The current scan shows two maxima, corresponding to the following electron transfer reactions at the electrode

$$Ru(bipy)_3^{3+} + e \rightleftharpoons Ru(bipy)_3^{2+} \ (E_p = +1.3V) \quad [10]$$

$$Ru(bipy)_3^{2+} + e \rightleftharpoons Ru(bipy)_3^{+} \ (E_p = -1.3V) \quad [11]$$

Homogeneous electron transfer between ionic species giving excited states occurs when the electrode potential becomes sufficiently negative to produce the reduced form of the ground state species; thus essentially all of the emission observed beyond -1.0V *vs.* SCE in this system can be attributed to annihilation. Some residual emission is seen, however, at high sensitivities at potentials where the concentration of the electrogenerated +1 reduced species should be quite small. For example, the concentration of $Ru(bipy)_3^{+}$ at the electrode surface at -1.3V *vs.* SCE is approximately 1.5 mmole; from the Nernst equation one calculates the concentration of $Ru(bipy)_3^{+}$ at the electrode surface at -0.5V. *vs.* SCE to be less than 2×10^{-13} mmole. This is too low to cause the residual emission observed at this potential. Thus this residual emission could not arise from homogeneous electron transfer but would necessarily arise from a preannihilation-type mechanism or conceivably, but not probably, by direct heterogeneous electron transfer at the metal electrode. Similar preannihilation emission was observed with all of the systems examined. Rigorous purification of solvent and supporting electrolyte would greatly reduce this emission but never entirely eliminate it, indicating at least some contribution to the ECL emission by impurities in the solvent and electrolyte.

Another possible approach to discriminate among the possible paths involves studying the time dependence of the ECL emission. Although attempts have been made to use the time dependence of the emission intensity during the potential step for this purpose (9, 10), the effects of possible quenching by radical ions and the complexity of the predicted annihilation results for triplet intermediates (2) suggest that unambiguous assignment by this approach may be difficult. An alternative method involves observation of the intensity decay following rapid current interruption. Qualitatively, under these conditions, the intensity would decay with the lifetime of the excited state for direct heterogeneous production. For homogeneous annihilation ECL the electrode would not reduce or oxidize the reactant ions at open circuit and the intensity decay should be governed by the rates of diffusion of the reactants.

Experimental results.—A summary of the results obtained using various compounds and semiconductor electrodes is given in Table II. For $TH^{+\cdot}$, $DPA^{+\cdot}$, and $Ru(bipy)_3^{3+}$, no emission which could be attributed unambiguously to direct heterogeneous production of excited states at the semiconductor electrodes was found. Either no emission was observed at potentials sufficient to produce excited states or the low levels of emission which were found at these potentials occurred at similar intensities and at the same potentials at a platinum electrode. Moreover, in these cases the decay times of the emission upon current interrup-

Table II. Summary of electrochemical and ECL data

Compound[a]	E_{T_1} (eV)	$E_{1/2}(R^{+\cdot}/R)$[b]	$E_{1/2}(R^{+\cdot}/^{3}R)$[b] (calc.)	Electrode	E_p[b,c]	Emission onset[b,d]
$Ru(bipy)_3^{3+}$	2.03[e]	1.30	−0.73	Pt	1.26	−0.5
				n-CdS	0.0	−0.6
				n-ZnO	−0.05	−0.65
				n-TiO_2	0.28	−0.6
$TH^{+\cdot}$	2.58[f]	1.23	−1.35	Pt	1.19	−1.9
				n-SiC	−0.75[i]	−2.0
				n-GaP	−0.95[i]	−2.0
$DPA^{+\cdot}$	1.8[g]	1.22	−0.58	Pt	1.18	−0.9
				n-ZnO	0.45	−0.9
				n-CdS	0.25	−0.9
$R^{+\cdot}$	1.2[h]	0.94	−0.26	Pt	0.90	−0.6
				n-TiO_2	−0.15	−0.7
				n-ZnO	0.45	−0.2
				n-CdS	−0.13	−0.25

[a] ACN solutions approximately 1 mmole compound and 0.1M TBAP ($TH^{+\cdot}$, $DPA^{+\cdot}$, and $R^{+\cdot}$ are radical cations of thianthrene, 9,10-diphenylanthracene, and rubrene, respectively).
[b] *V vs.* SCE.
[c] Reduction of compound. Cathodic current peak potential obtained by linear potential sweep voltammetry at 2 V/sec.
[d] Onset of ECL emission obtained with cathodic potential scans at 2 V/sec.
[e] Ref. (26).
[f] Ref. (27)
[g] Ref. (28).
[h] Ref. (29).
[i] Broad current peaks observed.

tion were much longer than those expected from the excited state lifetimes. These results suggest then that the observed emission at the semiconductor electrodes could be attributed mainly to preannihilation ECL rather than direct excited state formation. Different results were obtained upon reducing rubrene radical cation on n-CdS or n-ZnO, however. In these cases the behavior at platinum and at the semiconductors was very different and the ECL emission on current interruption showed unique and previously unobserved features. Details of these experiments are given below.

Because of the low solubility of R in ACN, ECL and electrochemical studies of R were carried out in benzonitrile (BZN) or in the mixed solvents benzene-BZN or benzene-ACN. A cyclic voltammogram of R in 0.1M TBAP/benzene-BZN is given in Fig. 3. R is reversibly oxidized and reduced in one electron transfer steps at 0.94 and −1.45V *vs.* SCE, respectively, in these solvent systems. Although phosphorescence of R has not been reported, energy transfer experiments indicate that the energy of the first triplet state is ~1.2 eV (23), approximately that of its parent molecule, naphthacene. Thus reduction of $R^{+\cdot}$ to the triplet state should occur at about −0.26V *vs.* SCE and n-TiO_2, n-ZnO, and n-CdS are suitable semiconductor electrodes to study the direct production of ^3R. Ideally the semiconductor electrodes should have a flatband potential, V_{fb}, negative of the potential needed to form the triplet, yet considerably removed from the thermodynamic potential for the reduction of R to $R^{-\cdot}$ to discriminate between reduction of $R^{+\cdot}$ to the excited triplet state and production of $R^{-\cdot}$ and annihilation ECL.

Current-potential curves for the reduction of $R^{+\cdot}$ at n-ZnO and n-CdS by linear single sweep voltammetry are given in Fig. 4. In the absence of intermediate levels or surface states within the bandgap region reduction of couples with redox potentials deep in the gap (*e.g.*, $R^{+\cdot}/R$ or $R^{+\cdot}/^3R$) should occur only at potentials near or negative of V_{fb}. However, studies of a number of redox couples in nonaqueous solutions at these semiconductors (20, 21) have shown reductions to occur significantly positive of V_{fb} at potentials characteristic of some intermediate levels or surface states. The current peak for the reduction of $R^{+\cdot}$ at about 0.5V *vs.* SCE (Fig. 4a) agrees quite well with the intermediate level proposed for n-ZnO (21). For potentials more negative than V_{fb}, the n-ZnO becomes degenerate, the electrode behavior approaches that of a metal (24) and reversible reduction of R to $R^{-\cdot}$ is observed.

The ECL intensity-potential profiles obtained during reduction of $R^{+\cdot}$ at Pt, n-CdS, and n-ZnO upon cathodic linear potential scans from potentials where $R^{+\cdot}$ is stable, well positive of the flatband potential of the semiconductor electrodes, are shown in Fig. 5. Note that reduction of $R^{+\cdot}$ on n-CdS and n-ZnO yields considerable emission at potentials positive of those where emission is observed on the platinum electrode. The potential sweep at the n-ZnO semiconductor electrode resulted in an emission peak at *ca.* −0.35V *vs.* SCE (in addition to the emission at *ca.* −1.5V due to the homogeneous ion annihilation reaction of $R^{+\cdot}$ and the $R^{-\cdot}$). Similarly, a peak at *ca.* −0.50V was obtained on the n-CdS semiconductor electrode. In both cases, the emission occurred at potentials where the triplet state is energetically just accessible yet at potentials positive of the flatband potential. This emission at rather positive potentials was quite reproducible over several hours and was found to be as large as 2-3% of the homogeneous annihilation

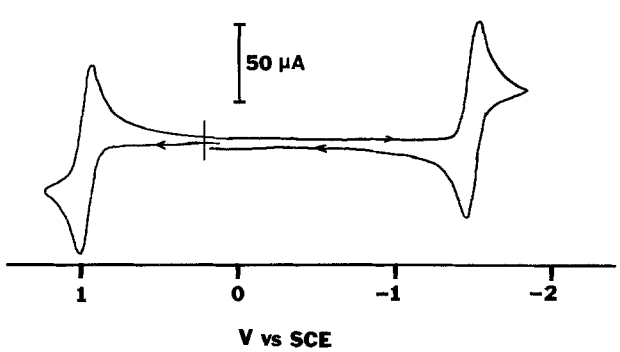

Fig. 3. Cyclic voltammogram of 1.5 mmoles R in 0.1M TBAP/benzene-BZN on platinum. Scan rate is 200 mV/sec.

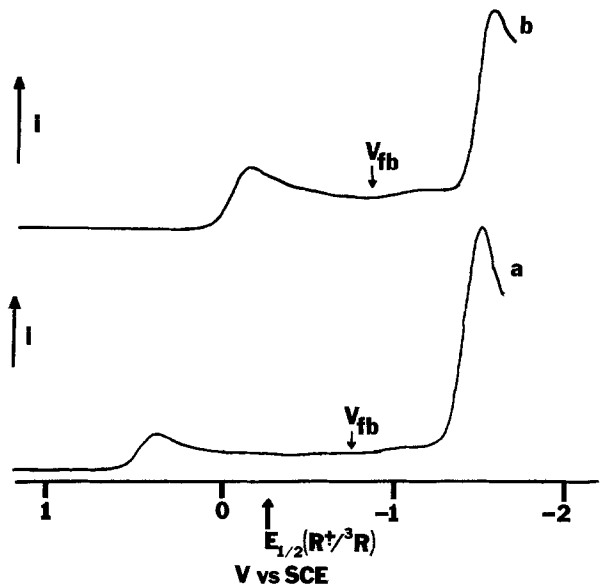

Fig. 4. Linear potential sweep voltammogram obtained with *ca.* 1 mmole $R^{+\cdot}$ in 0.1M TBAP/BZN on (a) n-ZnO, (b) n-CdS. Scan rate is 2 V/sec.

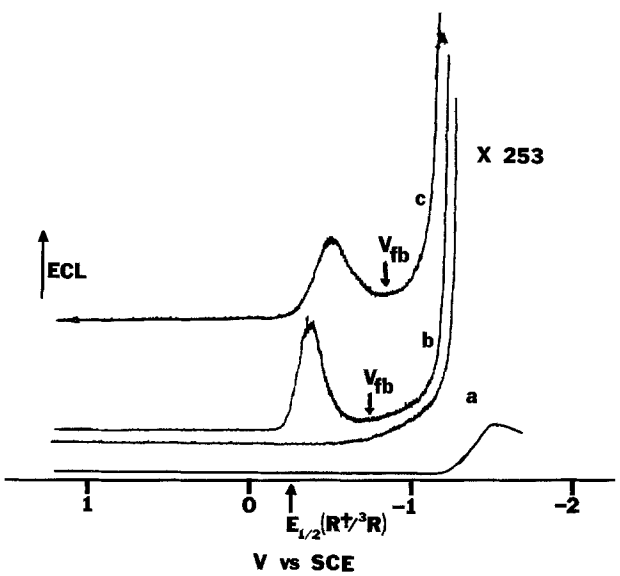

Fig. 5. ECL-potential profiles obtained with *ca.* 1 mmole $R^{+\cdot}$ in 0.1M TBAP solution at 2 V/sec. (a) Platinum electrode in benzene-ACN, (b) n-ZnO in benzene ACN, (c) n-CdS in BZN.

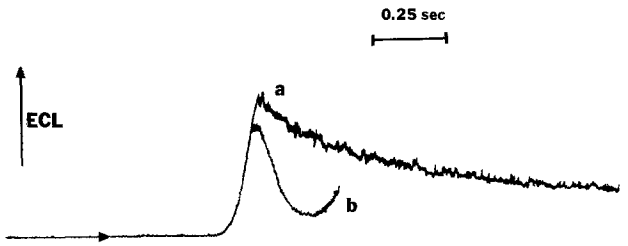

Fig. 6. ECL-time profile obtained concurrently with cathodic potential scan from 1.18V *vs.* SCE with *ca.* 1 mmole $R^{+\cdot}$ in 0.1M TBAP/BZN on n-CdS. Scan rate is 2 V/sec. (a) Potential ramp terminated at −0.5V *vs.* SCE (at curve maximum); (b) scan to −1.1V *vs.* SCE.

ECL emission produced at −1.5V under these conditions. That the peaked shape of the emission observed on the potential sweep at −0.35V (n-ZnO) and −0.50V (n-CdS) was caused by a potential, rather than a time, dependence was shown by the experiment of Fig. 6. When the potential ramp was stopped at potentials of the emission peak, the decay of the emission was rather slow (curve a). However, if the potential was scanned beyond the peak potential, the emission decayed abruptly (curve b).

To study the contribution to the emission by triplet states via triplet-triplet annihilation, the time dependence of the ECL emission was examined using a potential step excitation. Typical results obtained by stepping the potential from +1.1 to −0.7V *vs.* SCE at n-ZnO or to −0.62V at n-CdS are shown in Fig. 7. In both cases the cathodic current decay was proportional to $t^{-1/2}$, as expected for the diffusion-controlled reduction of $R^{+\cdot}$. The ECL intensity decay, however, was proportional to t^{-1}, or the square of the current, indicative of triplet generation followed by triplet-triplet annihilation (assuming a triplet lifetime controlled by quenching). Note that although a homogeneous annihilation production of ^3R could lead to a similar t^{-1} decay, the potentials employed in the step experiments preclude appreciable generation of $R^{-\cdot}$ and emission from the $R^{+\cdot}/R^{-}$ reaction route. In fact, potential steps to potentials where $R^{-\cdot}$ was generated at the semiconductor showed an emission decay with a dependence between $t^{-1/2}$ and t^{-1}.

Current interruption techniques were also informative and showed very different behavior for Pt and

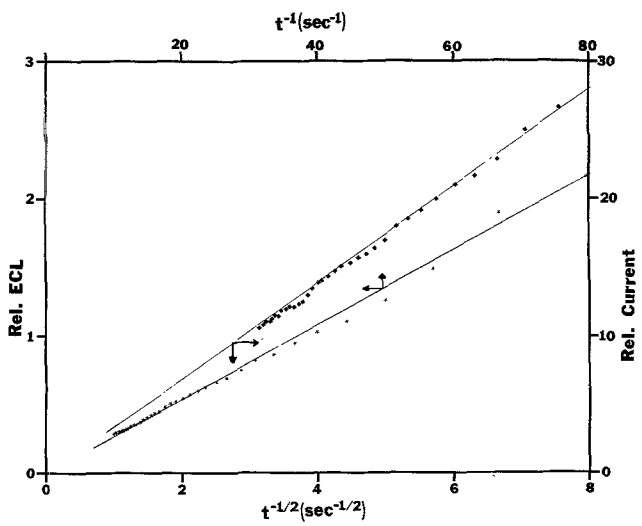

Fig. 7. ECL-time and current time profiles obtained with *ca.* 1 mmole $R^{+\cdot}$ in 0.1M TBAP/benzene-BZN by a cathodic potential step from +1.0V *vs.* SCE to −0.7V *vs.* SCE on n-ZnO. Current, ■; emission, *.

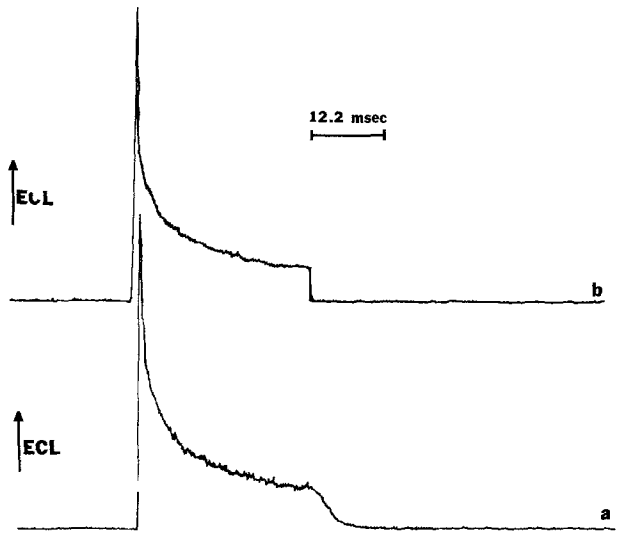

Fig. 8. ECL-time profiles obtained by cathodic potential steps to −1.1V *vs.* SCE with 1.5 mmoles $R^{+\cdot}$ in 0.1M TBAP/benzene-BZN on platinum. (a) Current interruption was employed after 30 msec. (b) Anodic potential step to 0.0V *vs.* SCE was employed after 30 msec.

the semiconductor electrodes. ECL intensity time curves for a Pt electrode for potential steps of 30 msec to −1.1V (the presumed preannihilation region) are shown in Fig. 8. When the current was interrupted at the end of the step (curve a), the emission decay time was *ca.* 5 msec. In contrast, when the potential was stepped back to +0.0V after the cathodic step the emission decay was much faster (*ca.* 5 μsec) (curve b). In this case, bringing the electrode potential to positive potentials caused oxidation of the species responsible for emission and probably also ^3R; this result suggests that the emission occurs at or very near the electrode surface. Very different results were obtained upon current interruption with the semiconductor electrodes; typical results are shown in Fig. 9 and 10. When the initial potential step was to a potential, E_1, corresponding to the emission peak (Fig. 9c or 10a), the emission showed a slow decay during the peak and a decay in 0.4-3.6 msec to zero upon interruption. However, when the potential was stepped to values beyond the emission peak (but before potentials where preannihilation ECl is observed) a large peak which rapidly decays to low emission intensities during the step is

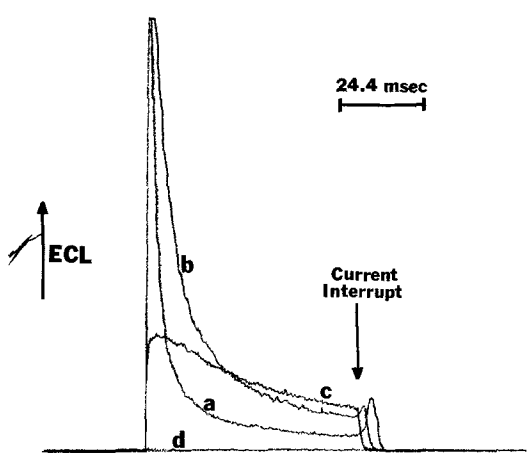

Fig. 9. ECL-time profiles obtained by cathodic potential steps n-CdS with *ca.* 1 mmole $R^{+\cdot}$ in 0.1M TBAP/BZN. Current interruption employed after 60 msec. Cathodic potential: (a) −0.92V *vs.* SCE, (b) −0.62V *vs.* SCE, (c) −0.47V *vs.* SCE, (d) −0.27V *vs.* SCE.

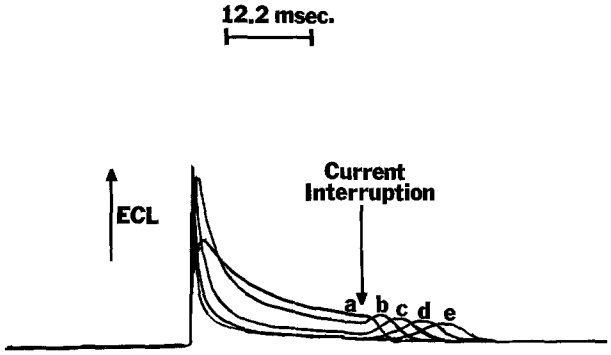

Fig. 10. ECL-time profiles obtained by cathodic potential steps on n-ZnO with $R^{+\cdot}$ in 0.1M TBAP/benzene-BZN. Current interruption was employed after 30 msec. Cathodic potential: (a) −0.3V *vs.* SCE, (b) −0.4V *vs.* SCE, (c) −0.5V *vs.* SCE, (d) −0.6V *vs.* SCE, (e) −0.7V *vs.* SCE.

observed (Fig. 9a and b, Fig. 10b-e). Upon interruption the emission decays or remains small for a time, but then a new emission peak, which occurs while the electrode is at open circuit, appears. This second, "echo" peak occurs at progressively later times after current interruption, the more negative is E_1. If, rather than using current interruption, the electrode was stepped to more positive potentials following the cathodic step, the emission would decay abruptly when the final potential was well positive of the emission peak potential (*e.g.*, 0.0V). However, when the second potential step was to a value at or near the emission peak, a second emission on the positive potential step occurred. Thus, for example, when $E_1 = -0.7$V on n-ZnO the effective decay time of emission on interruption was as long as 14 msec. However, when the potential was stepped to +1.1V, the emission decayed in about 95 μsec. Similar behavior was found with the semiconductor electrodes with triangular potential ramps (*i.e.*, cyclic voltammetry) (Fig. 11). When the scan direction was reversed following the emission peak, the emission again increased (although the cathodic current decreased on reversal) at potentials near the original emission maximum.

Discussion

The results obtained can be rationalized based on the known energetics of the rubrene system and the band structure of the semiconductors (Fig. 12). In this model there are different potential regions of the semiconductor electrode of interest. At positive potentials, just above the E° of the R^+/R couple, the number of electrons at the electrode-solution interface is small and no overlap between semiconductor levels and solution levels exists. Here no current flow or emission is observed. At somewhat more negative potentials the Fermi energy of the electrode is sufficient to populate an intermediate level or surface states, which leads to reduction of $R^{+\cdot}$ to the ground

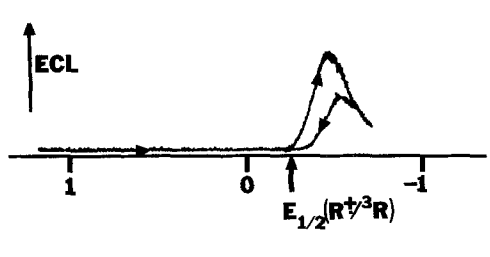

Fig. 11. ECL-potential profile obtained with concurrent cyclic voltammetry from +1.2V *vs.* SCE to −0.7V *vs.* SCE on n-CdS with *ca.* 1 mmole $R^{+\cdot}$ in 0.1M TBAP/BZN. Scan rate is 2 V/sec.

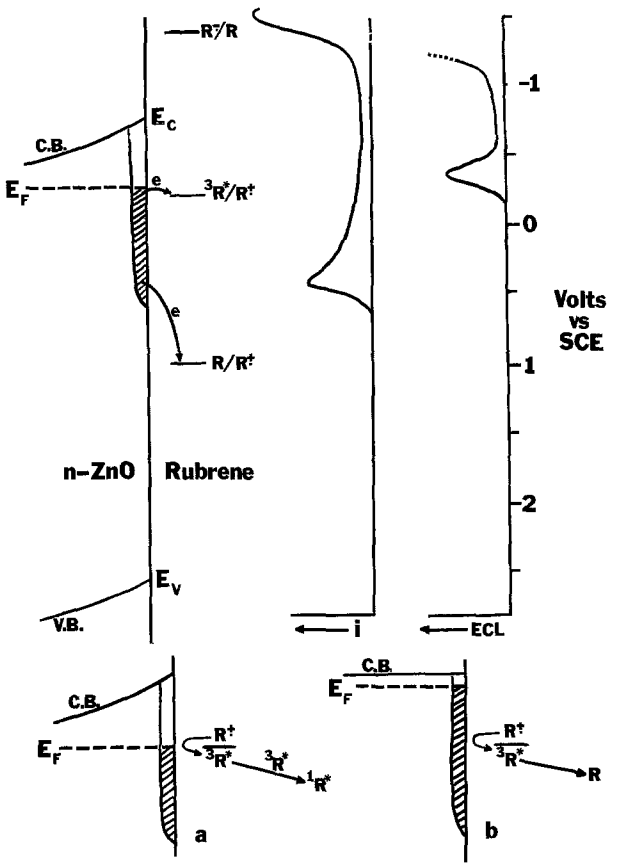

Fig. 12. Model for reduction of $R^{+\cdot}$ on n-ZnO. The current is proportional to the diffusion-limited reduction of $R^{+\cdot}$ to the ground state species and the ECL commences at potentials where $^3R^*$ is accessible (a) by electron transfer from the surface state. At more negative potentials (b) the excited states are more effectively quenched by the increased density of states at the electrode-solution interface.

state molecule, and a cathodic current is observed. The potential in this region is not sufficient to produce excited states, however. At more negative potentials the excited triplet species is thermodynamically accessible via surface states (the potential is still well positive of V_{fb}). Current continues to flow and is proportional to the flux of $R^{+\cdot}$ to the electrode. ECL emission is observed as the triplet species annihilate to yield the emitting singlet species. At still more negative potentials, however, as the surface states become more populated and the Fermi level approaches the conduction bandedge, the electrode becomes an effective quencher of the triplet states and the emission intensity increases. This explains the peak-shaped emission curve found on potential sweeps where the emission maximum occurs at potentials just at the $R^{+\cdot}/^3R$ potential. This model also explains the interruption experiments and the echo signals which appear at open circuit. Upon a potential step to potentials beyond the emission maximum the electrode is in a quenching mode and the emission decays to low levels. Upon interruption the Fermi level in the semiconductor begins to relax to that of the solution governed by the $R^{+\cdot}/R$ couple, by transfer of electrons to $R^{+\cdot}$ (coulostatic discharge). When E_F passes through the region of the $R^{+\cdot}/^3R$ potential, emission is observed. This potential drift was verified by independently monitoring the open-circuit potential of the n-ZnO electrode after a potential step to −0.93V *vs.* SCE followed by current

interruption. Thus, the time dependence of emission and the potential at open circuit monitors the rate of equilibration of the semiconductor electrode with the solution. The model further suggests that a semiconductor electrode can also act as an efficient quencher of excited states via surface or intermediate levels as well as via the conduction and valence band. The final potential region of interest is that well negative of V_{fb} where the electrode becomes degenerate. R^- is produced and emission via annihilation ECL in the bulk solution well away from the quenching electrode surface is observed.

That ECL emission by direct heterogeneous production of excited states on semiconductor electrodes is not observed with the other systems examined can also be rationalized by this model. The critical restraints for excited state production and emission on semiconductor electrodes are (*i*) the oxidized form of the parent-emitting species must be reducible at a surface state at energies within the gap at a potential to provide sufficient energy to populate the excited state species and (*ii*) this reduction must occur at potentials well positive of the flatband potential where the electrode is not degenerate and quenching by the electrode is less favorable. Competitive reductions of the oxidized species to ground state species by surface states must also be considered in evaluating the lack of observable ECL emission by the direct heterogeneous production of excited states on semiconductor electrodes in some systems. Moreover, evidence for direct excited state production probably requires a sufficiently stable oxidized species which is reducible to a triplet state undergoing triplet-triplet annihilation to form the emitting singlet, since direct reduction to a singlet state will frequently occur at potentials negative to V_{fb} and near potentials where annihilation ECL is possible. We conclude that it will be difficult to find many examples of direct excitation although the process is possible and that the efficiency of emission via this route will be small.

We might comment on other possible explanations for the results presented here. One might suggest production of ^3R via a discrete surface level of energy, E_T, which is only rapidly filled when E_F is near this level. At more negative potentials one would have to invoke a slower filling of the level and hence decreased emission, even when $E_F > E_T$. However, this model does not agree with past results on reductions of couples with potentials located in the gap region (20, 21), with the observed reduction of R^+ to the ground state at more positive potentials, and with the lack of perturbation of the cathodic current for potential steps into this region.

A second possible explanation for the potential dependence of the emission invokes the electrogeneration of quenchers at potentials just negative of where the emission is observed. In this case, however, the quencher concentration would be expected to be large enough after the cathodic potential step to diminish significantly the emission upon a subsequent anodic pulse or sweep. This is contrary to experimental observations. Moreover, the generation of quenchers might shift the emission potential or alter the emission peak shape in separate experiments at different rubrene concentrations, but this was not observed.

The model predicts that the quenching of excited states at a semiconductor electrode should be potential dependent and this could probably be tested in photoexcitation experiments. Moreover, observation of the rate of relaxation of an electrode at open circuit following a potential step may be useful in determining the extent to which surface states mediate electron transfer at the liquid/semiconductor junction.

Acknowledgment

The authors wish to thank Professor H. Gerischer for his enlightening conversations concerning this work and Paul Kohl for the flatband potential measurements. The support of this research by the Army Research Office is gratefully acknowledged.

Manuscript submitted March 21, 1978; revised manuscript received May 1, 1978.

Any discussion of this paper will appear in a Discussion Section to be published in the June 1979 JOURNAL. All discussions for the June 1979 Discussion Section should be submitted by Feb. 1, 1979.

Publication costs of this article were assisted by The University of Texas at Austin.

REFERENCES

1. T. Kuwana, in "Electroanalytical Chemistry," Vol. 1, A. J. Bard, Editor, chap. 3, Marcel Dekker, Inc., New York (1966).
2. A. J. Bard, K. S. V. Santhanam, S. A. Cruser, and L. R. Faulkner, in "Fluorescence," G. G. Guilbault, Editor, chap. 14, Marcel Dekker, New York (1966).
3. A. Zweig, *Adv. Photochem.*, **6**, 425 (1968).
4. E. A. Chandross, *Trans. N.Y. Acad. Sci., Ser. 2*, **31**, 571 (1969).
5. D. M. Hercules, *Acc. Chem. Res.*, **2**, 301 (1969).
6. D. M. Hercules, in "Physical Methods of Organic Chemistry," 4th ed., Part II, A. Weissberger and B. Rossiter, Editors, Academic Press, New York (1977).
7. A. J. Bard and L. R. Faulkner, in "Electroanalytical Chemistry," Vol. 10, A. J. Bard, Editor, chap. 1, Marcel Dekker, Inc., New York (1977).
8. L. R. Faulkner, in *MTP Int. Rev. Sci., Phys. Chem., Ser. Two*, **9** (1976).
9. M. Gleria and R. Memming, *Z. Phys. Chem.*, **101**, 171 (1976).
10. L. S. R. Yeh and A. J. Bard, *Chem. Phys. Lett*, **44**, 339 (1976).
11. E. A. Chandross and R. E. Visco, *J. Phys. Chem.*, **72**, 378 (1968).
12. R. A. Marcus, *ibid.*, **43**, 2654 (1965).
13. (a) R. R. Chance, A. Prock, and R. Sibley, *ibid.*, **60**, 2744 (1974); (b) K. H. Drexhage, H. Kuhn, and F. P. Schäfer, *Ber. Bunsenges. Phys. Chem.*, **72**, 329 (1968).
14. (a) A. Zweig, D. L. Maricle, J. S. Brinen, and A. H. Maurer, *J. Am. Chem. Soc.*, **89**, 473 (1967); (b) D. L. Maricle and A. H. Maurer, *ibid.*, **89**, 118 (1967).
15. R. E. Visco and E. A. Chandross, *Electrochim. Acta*, **13**, 1187 (1968).
16. D. M. Hercules, R. C. Lansbury, and D. K. Roe, *J. Am. Chem. Soc.*, **88**, 4578 (1966).
17. E. W. Grabner, *Electrochim. Acta*, **20**, 7 (1975).
18. R. Lansberg, P. Janietz, and R. Dehmlow, *J. Electroanal. Chem.*, **65**, 115 (1975).
19. S. M. Park and A. J. Bard, *J. Am. Chem. Soc.*, **97**, 2978 (1975).
20. S. N. Frank and A. J. Bard, *ibid.*, **97**, 7427 (1975).
21. P. A. Kohl and A. J. Bard, *ibid.*, **99**, 7531 (1977).
22. L. R. Faulkner, *This Journal*, **124**, 1724 (1977).
23. D. K. K. Liu and L. R. Faulkner, *J. Am. Chem. Soc.*, **99**, 4594 (1977).
24. J. F. Dewald, *Bell Syst. Tech. J.*, **39**, 615 (1960).
25. J. N. Demas and G. A. Crosby, *J. Mol. Spectrosc.*, **26**, 72 (1968).
26. F. E. Lytle and D. M. Hercules, *J. Am. Chem. Soc.*, **91**, 253 (1969).
27. J. M. Bonnier and R. Jardon, *J. Chim. Phys. Physiochim. Biol.*, **68**, 428 (1971).
28. S. L. Murov, in "Handbook of Photochemistry," p. 10, Marcel Dekker, New York (1973).
29. L. R. Faulkner, H. Tachikawa, and A. J. Bard, *J. Am. Chem. Soc.*, **94**, 691 (1972).